

AC

IC/95/359

CERN LIBRARIES, GENEVA



SCAN-9601117

300-1609

**INTERNATIONAL CENTRE FOR  
THEORETICAL PHYSICS**

**MULTICHANNEL APPROACH  
TO STUDYING SCALAR RESONANCES**

D. Krupa

V.A. Meshcheryakov

and

Yu.S. Surovtsev



**INTERNATIONAL  
ATOMIC ENERGY  
AGENCY**



**UNITED NATIONS  
EDUCATIONAL,  
SCIENTIFIC  
AND CULTURAL  
ORGANIZATION**

**MIRAMARE-TRIESTE**

International Atomic Energy Agency  
and  
United Nations Educational Scientific and Cultural Organization  
INTERNATIONAL CENTRE FOR THEORETICAL PHYSICS

**MULTICHANNEL APPROACH  
TO STUDYING SCALAR RESONANCES<sup>1</sup>**

D. Krupa

Institute of Physics, Slovak Academy of Science,  
Dúbravská cesta 9, 842 28 Bratislava, Slovakia.

V.A. Meshcheryakov<sup>2</sup>

International Centre for Theoretical Physics, Trieste, Italy

and

Yu.S. Surovtsev

Bogoliubov Laboratory of Theoretical Physics, Joint Institute for Nuclear Research,  
Dubna 141 980, Moscow Region, Russian Federation

MIRAMARE – TRIESTE

November 1995

<sup>1</sup>Submitted to Il Nuovo Cimento A.

<sup>2</sup>Permanent address: Bogoliubov Laboratory of Theoretical Physics, Joint Institute for Nuclear Research, Dubna 141 980, Moscow Region, Russian Federation.

## 1 INTRODUCTION

Analysis of low-energy experimental data has given interesting surprises [1] in spectroscopy of light mesons. One can see all the unexpectedness to be related mainly with the multichannel resonances. Above all, this concerns the scalar-meson sector. Therefore, the problem of getting reliable information about the multichannel resonances is more and more important at present. However, both the identification of such resonances and the determination of their QCD nature clash with a number of difficulties many of which are stimulated by considerable model-dependence of knowledge about these objects.

A model-independent consideration of resonances and their nature can be obtained on the basis of such general principles, as analyticity and unitarity, and the consistent balanced account of the nearest (to the considered physical region) singularities on all the relevant sheets of the Riemann surface of the  $S$ -matrix [2]-[6].

Developing our approach it is worth to concentrate on scalar mesons because there are no kinematical complications related with a spin, and moreover, practically all hypotheses (and even more, due to quantum numbers of vacuum [7]) about the nature of resonances concern also the scalar sector ( $qqq$ [8] – [10],  $gg$ [11],  $q\bar{q}$  [12, 13], the mixture of  $q\bar{q}$  and  $gg$  [14, 15] and the  $K\bar{K}$ -molecule [16, 17]). Note also the surviving intriguing situation in the 1 GeV-region of the scalar-isoscalar channel, where in the analysis of ISR data on central production of meson pairs ( $\pi\pi$  and  $K\bar{K}$ ) in  $pp$ -collisions [18], instead of the one  $f_0(980)$  meson three states were obtained:  $S_1(991)$ -a glueball candidate,  $S_2(988)$ -a  $K\bar{K}$  molecule,  $f_0(900)$ -a meson broad enough in  $\pi\pi$ -channel. Though after their subsequent enlarged analysis of the above data and also of data on  $\pi\pi$  and  $K\bar{K}$  scattering and on decays  $J/\psi \rightarrow \phi\pi\pi(\phi K\bar{K})$ ,  $D_s \rightarrow \pi\pi\pi$ , the authors of work [18] seem to be inclined to one resonance scenario for  $f_0(980)$  [19], but also the previous situation is discussed in literature, especially, in connection with an interesting possibility of supercritical confinement and “novel” hadrons [7].

Although it was already clear that the multichannel resonance is represented by pole clusters on the Riemann surface [2],[5], [19], the standard clusters were not yet determined. This is important for identification of resonances. Here, we perform this and indicate the reasons for of deviation from standard clusters related with the influence of closed channels

on forming the resonance and with the neglect of the threshold of a coupled channel.

## 2 $N$ COUPLED CHANNELS FORMALISM

Considering the multichannel problem, we pursue two aims: i. to obtain a model independent information about multichannel resonances and an indication about their QCD nature; ii. to describe the experimental data on the coupled processes. The first purpose is achieved provided the nearest (to the physical region of interest) singularities of the  $S$ -matrix are taken into account, and one can see that in this respect an  $N = 3$  channel problem can be effectively reduced to the 2- and 3-channel problem. However, to realize the second task, the general  $N$ -channel formalism can be useful

1. Consider the  $N$  channel  $S$ -matrix (all channels are two-particle ones) determined on the  $2^N$ -sheeted Riemann surface. The latter have the right-hand (unitary) cuts along the real axis of the  $s$ -variable complex plane  $(4m_i^2, \infty)$  ( $i = 1, 2, \dots, N$  means a channel through which the physical sheet is sewed together with other corresponding sheets). The branch points are at the vanishing values of the channel momenta

$$k_\alpha = (s/4 - m_\alpha^2)^{1/2}.$$

For the time being, the left-hand (potential) cuts, which are related with the crossing channel contributions, will be neglected in the Riemann-surface structure and their contributions will be taken into account in the background of the corresponding amplitudes.

It is convenient to use the following enumeration of sheets (see, e.g. [20]), we shall denote the physical sheet as  $L_0$  and other sheets through  $L_{i_1 \dots i_k}$ , where  $i_1, \dots, i_k$  are a system of subscripts of those channel-momenta  $k_{i_n}$  which change signs at analytical continuations from the physical sheet onto the indicated one.

Express the analytical continuations of  $S$ -matrix elements to the unphysical sheets  $S_{i_1 \dots i_k}^{(i_1 \dots i_k)}$  in terms of them on the physical sheet  $S_{i_1 \dots i_k}^{(0)}$ , using the reality of the analytical functions and the  $N$ -channel unitarity. To this end, first, we shall introduce the notation:  $\mathbf{S}^{[i_1 \dots i_k]}$  means a matrix in which all the rows are composed of the vanishing elements but the rows  $i_1, \dots, i_k$ , that consist of elements  $S_{i_n m_n}$ . In the matrix  $\mathbf{S}^{(i_1 \dots i_k)}$ , on the contrary

the rows  $i_1, \dots, i_k$  are zeros. Therefore,

$$\mathbf{S}^{[i_1 \dots i_k]} + \mathbf{S}^{(i_1 \dots i_k)} = \mathbf{S}.$$

Further  $\mathbf{\Delta}^{[i_1 \dots i_k]}$  and  $\mathbf{\Delta}^{(i_1 \dots i_k)}$  denote the diagonal matrices with zero nondiagonal elements and with the diagonal ones

$$\Delta_{ii}^{[i_1 \dots i_k]} = \begin{cases} 1 & \text{if } i \in (i_1 \dots i_k), \\ 0 & \text{for remaining } i, \end{cases} \quad \text{and} \quad \Delta_{ii}^{(i_1 \dots i_k)} = \begin{cases} 0 & \text{if } i \in (i_1 \dots i_k), \\ 1 & \text{for remaining } i, \end{cases}$$

respectively. Then the analytical continuations of the  $S$ -matrix to the sheet  $L_{i_1 \dots i_k}$  will be represented as

$$\mathbf{S}^{(i_1 \dots i_k)} = \frac{\mathbf{S}^{(0)(i_1 \dots i_k)} - i\mathbf{\Delta}^{[i_1 \dots i_k]}}{\mathbf{\Delta}^{(i_1 \dots i_k)} - i\mathbf{S}^{(0)[i_1 \dots i_k]}}, \quad (1)$$

from which the corresponding relations for the  $S$ -matrix elements can be derived by the formula for the matrix division.

Generally, the obtained formula (1) is a solution of the  $N$ -channel problem in the sense of giving a chance to predict (on the basis of analysis of one process) the coupled-process amplitudes on the uniformization plane of the  $S$ -matrix at a certain conjecture about the background. Let us demonstrate this on the basis of the 2- and 3-channel problems.

Consider the 3-channel problem and, for definiteness, the channels:  $\pi\pi - 1$ ,  $K\bar{K} - 2$ ,  $\eta\eta - 3$ . It is clear that the elements of the 3-channel  $S$ -matrix  $S_{ik}$ , where  $i, k = 1, 2, 3$ , have the right-hand (unitary) cuts along the real axis of the  $s$ -variable complex plane starting at  $4m_\pi^2$ ,  $4m_K^2$ ,  $4m_\eta^2$  (as it is mentioned above, the left-hand cuts will be neglected for the present in the Riemann-surface structure), and the  $S$ -matrix is determined on the 8-sheeted Riemann surface. Then, using formula (1), we derive the analytical continuations of the  $S$ -matrix elements to the unphysical sheets [6] (Table 1: index “(0)” is omitted; besides the notation of the Riemann-surface sheets accepted here, their notation by the Roman numerals which has been used in our previous works [2]-[6] is indicated;  $D_{ij}$  are the minors corresponding to the  $S$ -matrix element  $S_{ij}$ , for example,  $D_{11} = S_{22}S_{33} - S_{23}^2$ ,  $D_{22} = S_{11}S_{33} - S_{13}^2$ ,  $D_{23} = S_{11}S_{23} - S_{12}S_{13}$ , etc.). The left upper subtable of Table 1, corresponding to the processes  $1 \rightarrow 1$ ,  $1 \rightarrow 2$ ,  $2 \rightarrow 2$  and to the sheets  $L_0$  (I),  $L_1$  (II),  $L_{12}$  (III),  $L_2$  (IV), gives the 2-channel problem. Now one can see from

Table 1.

	$L_0$	$L_1$	$L_{12}$	$L_2$	$L_{23}$	$L_{123}$	$L_{13}$	$L_3$
	I	II	III	IV	V	VI	VII	VIII
$1 \rightarrow 1$	$S_{11}$	$\frac{1}{S_{11}}$	$\frac{S_{22}}{D_{33}}$	$\frac{D_{33}}{S_{22}}$	$\frac{\det S}{D_{11}}$	$\frac{D_{11}}{\det S}$	$\frac{S_{33}}{D_{22}}$	$\frac{D_{22}}{S_{33}}$
$1 \rightarrow 2$	$S_{12}$	$\frac{iS_{12}}{S_{11}}$	$-\frac{S_{12}}{D_{33}}$	$\frac{iS_{12}}{S_{22}}$	$\frac{iD_{12}}{D_{11}}$	$-\frac{D_{12}}{\det S}$	$\frac{iD_{12}}{D_{22}}$	$\frac{D_{12}}{S_{33}}$
$2 \rightarrow 2$	$S_{22}$	$\frac{D_{33}}{S_{11}}$	$\frac{S_{11}}{D_{33}}$	$\frac{1}{S_{22}}$	$\frac{S_{33}}{D_{11}}$	$\frac{D_{22}}{\det S}$	$\frac{\det S}{D_{22}}$	$\frac{D_{11}}{S_{33}}$
$1 \rightarrow 3$	$S_{13}$	$\frac{iS_{13}}{S_{11}}$	$-\frac{iD_{13}}{D_{33}}$	$-\frac{D_{13}}{S_{22}}$	$-\frac{iD_{13}}{D_{11}}$	$\frac{D_{13}}{\det S}$	$-\frac{S_{13}}{D_{22}}$	$\frac{S_{13}}{S_{33}}$
$2 \rightarrow 3$	$S_{23}$	$\frac{D_{23}}{S_{11}}$	$\frac{iD_{23}}{D_{33}}$	$\frac{iS_{23}}{S_{22}}$	$-\frac{S_{23}}{D_{11}}$	$-\frac{D_{23}}{\det S}$	$\frac{iD_{23}}{D_{22}}$	$\frac{S_{23}}{S_{33}}$
$3 \rightarrow 3$	$S_{33}$	$\frac{D_{22}}{S_{11}}$	$\frac{\det S}{D_{33}}$	$\frac{D_{11}}{S_{22}}$	$\frac{S_{22}}{D_{11}}$	$\frac{D_{33}}{\det S}$	$\frac{S_{33}}{D_{22}}$	$\frac{1}{S_{33}}$

Table 1 how the singularities and zeros of the one-process amplitude (e.g.  $S_{11}$ ) on all the Riemann-surface sheets are carried over to the corresponding sheets for other amplitudes of the coupled scattering processes determining completely the latter in the considered energy region. In practice this can be realized on the uniformization plane of the  $S$ -matrix.

To derive, by this method, the matrix elements of the processes of transitions between channels ( $S_{ij}$ ,  $i \neq j$ ), one should consider the analytical continuations of the expressions  $S_{ii}S_{jj} - S_{ij}^2$  to all sheets. With Table 1, this can be easily made in terms of simple algebraic operations (Table 2), and one can see that one amplitude of scattering ( $S_{11}$ ) determines also the transition amplitudes. This method has been applied by us in the 2-channel approach [4]) for obtaining the  $K\bar{K}$  scattering amplitude and the prediction on the  $\pi\pi \rightarrow K\bar{K}$  process on the basis of data on  $\pi\pi$  scattering. For this, in addition to uniformization of the  $S$ -matrix, it was necessary to use a certain representation of multichannel resonances on the Riemann surfaces.

Table 2.

	$L_0$	$L_1$	$L_{12}$	$L_2$	$L_{23}$	$L_{123}$	$L_{13}$	$L_3$
	I	II	III	IV	V	VI	VII	VIII
$S_{11}S_{22} - S_{12}^2 = D_{33}$		$\frac{S_{22}}{S_{11}}$	$\frac{1}{D_{33}}$	$\frac{S_{11}}{S_{22}}$	$\frac{D_{22}}{D_{11}}$	$\frac{S_{33}}{\det S}$	$\frac{D_{11}}{D_{22}}$	$\frac{\det S}{S_{33}}$
$S_{11}S_{33} - S_{13}^2 = D_{22}$		$\frac{S_{33}}{S_{11}}$	$\frac{D_{11}}{D_{33}}$	$\frac{\det S}{S_{22}}$	$\frac{D_{33}}{D_{11}}$	$\frac{S_{22}}{\det S}$	$\frac{1}{D_{22}}$	$\frac{S_{11}}{S_{33}}$
$S_{22}S_{33} - S_{23}^2 = D_{11}$		$\frac{\det S}{S_{11}}$	$\frac{D_{22}}{D_{33}}$	$\frac{S_{33}}{S_{22}}$	$\frac{1}{D_{11}}$	$\frac{S_{11}}{\det S}$	$\frac{D_{33}}{D_{22}}$	$\frac{S_{22}}{S_{33}}$

2) The latter issue can be clarified but again with formulae (1) (in particular, Tables 1 and 2) expressing the analytical continuations of the  $S$ -matrix elements to the unphysical sheets in terms of them on the physical sheet. These expressions are suitable because the matrix elements on the physical sheet  $L_0$  have, except for the real axis, only zeros corresponding to resonances, at least, around the physical region.

Provided a resonance has the only decay mode (1-channel case), the general statement about a behaviour of the process amplitude is that at energy values in a proximity to the resonant one it describes the propagation of a resonance as if the latter were a free particle. This means that in the matrix element the resonance (in the limit of its narrow width) is represented by a pair of complex conjugate poles on the sheet  $L_1$  and by a pair of conjugate zeros on the physical sheet at the same points of complex energy. This model-independent statement about the poles as the nearest singularities holds also when taking account of the finite width of a resonance.

In the 2-channel case, formulae of Table 1 immediately give the resonance representation by poles and zeros on the 4-sheeted Riemann surface. Here one must discriminate between three types of resonances which are described: (a) by a pair of complex conjugate poles on the sheet  $L_1$  and therefore by a pair of complex conjugate zeros on the sheet  $L_0$  in  $S_{11}$ , (b) by a pair of conjugate poles on the sheet  $L_2$  and therefore by a pair

of complex conjugate zeros on  $L_0$  in  $S_{22}$ . **(c)** by one pair of conjugate poles on each of sheets  $L_1$  and  $L_2$ , that is by one pair of conjugate zeros on the physical sheet in each of matrix element  $S_{11}$  and  $S_{22}$ .

To the resonances of types **(a)** and **(b)** one has to make correspond a pair of complex conjugate poles on the sheet  $L_{12}$  which are shifted relative to a pair of poles on the sheet  $L_1$  and  $L_2$ , respectively (if the coupling among channels were absent, i.e.  $S_{12} = 0$ , the poles on  $L_{12}$  would lay exactly **(a)** under the poles on  $L_1$ , **(b)** above the poles on the sheet  $L_2$ ). To the resonances of type **(c)** one must make correspond two pairs of conjugate poles on  $L_{12}$  which are reasonably expected to be a pair of the complex conjugate compact formations of poles. Thus, here we have three types of resonance clusters.

In the 3-channel problem, formulae of Table 1 give the resonance representation on the 8-sheeted Riemann surface. Here, one must distinguish seven types of resonances (respectively seven clusters) with zeros on the physical sheet in **(a)**  $S_{11}$ , **(b)**  $S_{22}$ , **(c)**  $S_{33}$ , **(d)**  $S_{11}$  and  $S_{22}$ , **(e)**  $S_{22}$  and  $S_{33}$ , **(f)**  $S_{11}$  and  $S_{33}$ , **(g)**  $S_{11}$ ,  $S_{22}$  and  $S_{33}$ . For example, in the case of the resonance of type **(g)** there are one pair of complex conjugate poles on each of sheets  $L_1$ ,  $L_2$  and  $L_3$  at the same points of  $s$ -variable where the zeros lie on  $L_0$ , also two pairs of complex conjugate poles on each of sheets  $L_{12}$ ,  $L_{23}$  and  $L_{13}$ , and three pairs of complex conjugate poles on  $L_{123}$  (i.e. the resonance is represented by complex conjugate clusters of poles and zeros).

Generally, in the  $N$ -channel problem, when zeros corresponding to the  $N$ -channel resonance are present on the sheet  $L_0$  in the  $S$ -matrix elements, for example, at an  $N$ -considered coupled processes of scattering  $S_{ii}$ , there are one pair of conjugate poles on each of the sheets  $L_k$  ( $k = 1, \dots, N$ ), two pairs of conjugate poles on each of the sheets  $L_{ij}$ , three pairs of poles on the sheets  $L_{ijk}$ , etc. and, finally,  $N$  pairs of poles on the sheet  $L_{1\dots N}$ . However, the first two considered (2- and 3-channel) cases seems to exhaust the multichannel-resonance division into types (as model-independent characteristics), because always the problem of the representation of the  $N$  ( $> 3$ )-channel resonances by the nearest singularities can be effectively reduced to the above cases which give the standard resonance clusters of poles and zeros on the Riemann surfaces. Note also that this resonance division into types is not formal. For instance, in the scalar meson, see

for the resonance  $f_0(975)$  seems to correspond to type **(a)**, and the resonance  $f_0(1590)$  corresponds to one of types without zeros on  $L_0$  in  $S_{11}$ . These two resonances have very different QCD natures. Further investigation of this matter can possibly give rise to the model-independent indications of the multichannel-resonance nature on the basis of their pole representation on the Riemann surfaces.

3. Let us indicate one reason that causes a deviation from standard clusters describing the resonance. Consider the  $K$ -matrix in the  $N$ -channel case which is related with the  $S$ -matrix as follows

$$\mathbf{S} = \frac{I + i\rho^{1/2}\mathbf{K}\rho^{1/2}}{I - i\rho^{1/2}\mathbf{K}\rho^{1/2}}, \quad (2)$$

where  $\rho_{ij} = 0$  ( $i \neq j$ ),  $\rho_{ii} = 2k_i/\sqrt{s}$ . From (2) it is easy to obtain that  $\mathbf{K} = \mathbf{K}^+$ , i.e., the  $K$ -matrix has no discontinuity when going across the two-particle unitary cuts, and the poles corresponding to a resonance lie on the real axis. The sole pole on the real axis corresponds to a resonance of the simplest type (only with the sole pair of complex conjugate poles on each of the corresponding sheets, i.e. with a pair of zeros on sheet  $L_0$  only in the one-matrix element  $S_{ii}$ ). Resonances **(c)** in the 2-channel case and **(d)**, **(e)**, **(f)** in the 3-channel case are described by two poles in the  $K$ -matrix. Resonance **(g)** has three poles.

However, the many-pole representation of a resonance in the  $K$ -matrix arises also as a result of influence of the important energetical-closed channels. Let us explain this in more detail. In practice we deal usually with a reduced  $K$ -matrix,  $\mathbf{K}_R$ , corresponding to the  $M$  open channels whereas the remaining  $N - M$  channels are energetical-closed. A connection between the reduced matrix  $\mathbf{K}_R$  and the complete  $K$ -matrix is given by [21]

$$(\mathbf{K}_R)_{ij} = K_{ij} + iK_{i\alpha}[(I - i\hat{\rho}\hat{\mathbf{K}})^{-1}\hat{\rho}]_{\alpha\beta}K_{\beta j}. \quad (3)$$

Here  $\hat{\rho}$  and  $\hat{\mathbf{K}}$  denote the submatrices being related to the closed channels,  $i, j = 1, \dots, M$  refer to open channels and  $\alpha, \beta = M + 1, \dots, N$  correspond to closed ones. It is clear that the resonances can arise both owing to the resonant interaction of particles in the open channels and by virtue of the processes in the closed channels. In the first case, each element of the complete  $K$ -matrix has a pole at a certain real value of energy  $s = m^2$ . In

proximity to this pole one can write

$$K_{\sigma\tau} = \frac{g_\sigma g_\tau}{s - m^2} + \alpha_{\sigma\tau}(s), \quad (1)$$

where  $g_\sigma, g_\tau$  are constants of the resonance couplings with particles of open and closed channels ( $\sigma, \tau = 1, \dots, N$ ),  $\alpha_{\sigma\tau}(s)$  are the background smooth functions. However this pole is absent in the  $K_R$ -matrix, since the residue at this pole in (3) is equal to zero, and the position of a pole corresponding to a resonance is renormalized due to the influence of the closed channels, moreover the resonance is described by a number of poles. For example, at the conjecture of negligible background ( $\alpha_{\sigma\tau} = 0$ ) we obtain from (3) with (4):

$$(K_R)_{ij} = \frac{g_i g_j}{s - m^2 + \sum_{\alpha=M+1}^N g_\alpha^2 |\rho_\alpha|}. \quad (5)$$

Consideration of the background does not change the conclusion about the pole at  $s = m^2$ . For instance, in the 2-channel case with closed channel 2 we should have, with the background,

$$(K_R)_{11} = \frac{g_1^2(1 + |\rho_2|\alpha_{22}) - |\rho_2|[2g_1 g_2 \alpha_{12} + (s - m^2)\alpha_{12}^*]}{s - m^2 + |\rho_2|[g_2^2 + (s - m^2)\alpha_{22}]} \quad (6)$$

From (5) and (6) one can see that only when a resonance is not coupled with closed channels in the  $K_R$ -matrix there is a pole at  $s = m^2$ . But even at small couplings of a resonance with particles of closed channels the resonance is represented by a number of poles. A successive explicit consideration of a larger number of channels would reduce the number of poles corresponding to the given multichannel resonance. In particular, for the 2-channel resonance in the 1-channel consideration (formula (6)) at least two poles on the real axis in the vicinity of  $m^2$  describe this resonance. In the 2-channel consideration (for the “complete”  $K$ -matrix) there would be, of course, one pole at  $s = m^2$ , as distinct from the above-discussed case with a resonance (c). To understand this situation, we should investigate the pole representation of resonances on the Riemann surfaces.

Note that, as is seen from (3), a pole in the  $K_R$ -matrix may arise also in the case when the elements of complete  $K$ -matrix are nonsingular. The condition for this pole is that

$$\det(I + |\hat{\rho}|\hat{\mathbf{K}}) = 0. \quad (7)$$

This pole in the  $K_R$ -matrix exists, e. g., if particles in the lowest closed channel attract each other strongly enough to form a bound state provided the coupling between the

closed and open channel is weak. Notice, however, that the same condition (7) is required for existing the resonances due to processes both in the open and closed channels. To distinguish these cases, one must again study the pole arrangement on the Riemann surface.

4. So, using formula (1) one can obtain the representation of multichannel resonances on the Riemann surfaces and all the coupled-process amplitudes on their uniformization plane through analyzing one of them [4]. However, it is convenient (especially, meaning to carry out, in future, the joint analysis of the data on amplitudes the coupled processes) to use the Le Couteur–Newton relations [22] expressing the  $S$ -matrix elements of all coupled processes in terms of the Jost matrix determinant  $d(k_1, \dots, k_N) \equiv d(s)$  being a real analytical function with the only square-root branch-points at the process thresholds  $k_i = 0$ :

$$S_{ii}(s) = \frac{d^{(i)}(s)}{d(s)}, \quad (8)$$

$$\begin{vmatrix} S_{i_1 i_1}(s) & \dots & S_{i_1 i_k}(s) \\ \vdots & \ddots & \vdots \\ S_{i_k i_1}(s) & \dots & S_{i_k i_k}(s) \end{vmatrix} = \frac{d^{(i_1 \dots i_k)}(s)}{d(s)}. \quad (9)$$

The analytical structure of the  $S$ -matrix on all Riemann sheets given by formula (1) is thus expressed in a compact way by these relations. The real analyticity implies

$$d(s^*) = d^*(s) \quad (10)$$

for all  $s$ , and the unitarity condition requires further restrictions on the  $d$ -function for physical  $s$ -values which will be discussed below in the examples of 2- and 3-channel  $S$ -matrices. Further, in our approach of a consistent account of the nearest (to the considered physical region) singularities on all the relevant Riemann sheets, one should find a  $w$ -variable uniformizing the  $d$ -function on the  $w$ -plane. When there are more than two unitarity branch-points, this is impossible to do with the help of simple functions. Therefore, one can act as we shall do below in the 3-channel approach, namely, construct (if possible) a model of the Riemann surface approximating the initial Riemann surface in accordance with our approach and suitable for mapping onto a plane. In the last resort, there exists

always a possibility of the local uniformization, though in this case a parametrization may turn out to be not simple. Then the  $d$ -function can be represented as

$$d = d_B d_{res}, \quad (11)$$

where  $d_{res}(w)$  is responsible for describing the resonance or bound states and contains only zeros corresponding to these states (the kinematical poles can be present only at the point  $w = 0$ ). The function  $d_B$  describes the background and in the general case is of the form:

$$d_B = \varphi(s) \exp\left\{-i \sum_{k=1}^N \delta_k^B(q_k)\right\}. \quad (12)$$

Here  $\varphi$  is a certain analytical function, and  $\delta_k^B$  is the phase shift of the elastic part of the background in the  $k$ -th channel:

$$\delta_k^B(-q_k) = -\delta_k^B(q_k).$$

For the channel with the relative angular momentum  $l$ , one can take

$$\delta_k^B(q_k) = a q_k^{2l+1}.$$

Then, for example, for the  $m$ -th channel we obtain

$$S_{mm} = \frac{\varphi^{(m)}(s)}{\varphi(s)} e^{2i\delta_m^B(q_m)} \frac{d_{res}^{(i)}}{d_{res}}, \quad (13)$$

where  $\varphi^{(m)}(s)/\varphi(s)$  is the elasticity parameter of the background in the  $m$ -th channel, for the completely elastic background it is equal to one.

### 3 ANALYSIS OF EXPERIMENTAL DATA

#### 1. The 2-channel approach.

We have applied this method before to the 2-channel consideration [4], [6] of the experimental isoscalar  $s$ -wave of the  $\pi\pi$  scattering from the threshold to 1.9 GeV. The uniformizing variable used

$$z = (k_1 + k_2)/(m_K^2 - m_\pi^2)^{1/2} \quad (14)$$

maps the whole 4-sheeted Riemann surface onto the  $z$ -plane (Fig.1). On  $z$ -plane the Le

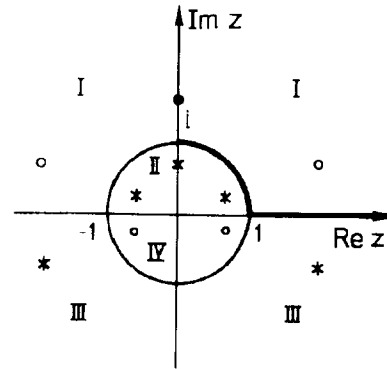


Fig.1: Plane of the uniformizing variable  $z$ . The Roman numerals (I, ..., IV) denote images of the corresponding sheets of the Riemann surface; the thick line represents the physical region (the points  $i$  and  $-i$  are the  $\pi\pi$  and  $K\bar{K}$  thresholds, respectively). The depicted positions of poles (\*) and of zeros (o) give the representation of the type (a) resonance in  $S_{11}$ . The pole and zero on the imaginary axis approximate the background.

Coutour-Newton relations are [4, 20]

$$S_{11} = \frac{d(-z^{-1})}{d(z)}, \quad S_{22} = \frac{d(z^{-1})}{d(z)}, \quad S_{11}S_{22} - S_{12}^2 = \frac{d(-z)}{d(z)}, \quad (15)$$

Then the condition of the real analyticity implies

$$d(-z^*) = d^*(z) \quad (16)$$

for all  $z$ , and the 2-channel unitarity requires the following relations to hold for the physical  $z$  values:

$$|d(-z^{-1})| \leq |d(z)|, \quad |d(z^{-1})| \leq |d(z)|, \quad |d(-z)| = |d(z)|. \quad (17)$$

The  $d$  function has been taken as  $d = d_B d_{res}$ , where

$$d_B = iz^{-1}(1 + iy_0z) \quad (18)$$

describes the background, and the resonance part has the form

$$d_{res} = z^{-2M} \prod_{n=1}^M (1 - z_n^* z)(1 + z_n z)(1 - z_n'^* z)(1 + z_n' z) \quad (19)$$

with  $M$  being the number of resonances,  $z_n$  and  $z_n'$  denoting the positions of zeros of  $S_{11}$  for the type (a) resonance "n" on the upper and lower  $z$ -half-plane, respectively (one value of the index  $n$  corresponds to one resonance). Now it is easy to obtain an expression for  $S_{11}$  and the amplitudes of other coupled processes. As is known, the  $\pi\pi$  interaction is practically elastic up to the  $K\bar{K}$  threshold, the contribution of the multiparticle states

$(4\pi, 6\pi)$  is negligible within the up-to-date experiment accuracy. This property of the  $\pi\pi$ -interaction is satisfied by the background (18) and by the resonance part (19) (see Fig.1) due to the symmetry of the poles and zeros with respect to the unit circle. If the  $\pi\pi$ -scattering were elastic also above the  $K\bar{K}$  threshold, there would be the symmetry of the poles and zeros with respect to the real axis. The symmetry of the whole picture relative to the imaginary axis ensures the property of the real analyticity. The function  $d_{B^0}$  of the form (19) gives resonances of the type **(a)**. Modifications for the resonances of other types are evident from the discussion in section 1.1 and Table 1.

With formulae (15)-(19) we have analyzed the  $\pi\pi$ -scattering data in the energy regions 0.6-1.89 GeV and from the threshold to 1.89 GeV [4]-[6]. In the first case the data of work [23] are used, in the second case the experimental points of many works [23, 24] available are taken. In both the cases, we have obtained a satisfactory description ( $\chi^2/\text{ndf} \approx 1.00$  and  $\chi^2/\text{ndf} \approx 1.04$ , respectively) of the phase shift  $\delta_0^0$  and the elasticity parameter  $\eta_0^0$  with two resonances of the type **(a)** ( $f_0(975)$  and  $f_0(1500)$ ). The following zero positions on the  $z$ -plane corresponding to resonances "1" and "2" have been established in the first analysis (0.6-1.89 GeV):

$$z_1 = 1,2281 + 0,15318i, \quad z'_1 = 0,72984 - 0,24186i,$$

$$z_2 = 2,8933 + 0,59804i, \quad z'_2 = 0,34796 - 0,05662i,$$

(zero corresponding to the background,  $y_0 = 1,2634$ ).

in the second analysis (from the threshold to 1.89 GeV):

$$z_1 = 1,2083 + 0,17813i, \quad z'_1 = 0,34163 - 0,14893i,$$

$$z_2 = 3,1173 + 0,85304i, \quad z'_2 = 0,31332 - 0,097095i,$$

( $y_0 = 4,2928$ ).

So, in these analyses, the influence of the  $K\bar{K}$  threshold is taken into account explicitly with the help of uniformizing variable  $z$ . However, in the analysed energy region, there are the threshold of the  $\eta\eta$  channel, considerable couplings with which of the investigated resonances are indicated by many quark models, and thresholds of other channels ( $\eta\eta', \rho\rho, \omega\omega$ ), with which these resonances may be coupled. To take account of their effects and also the effects of such phenomena, as the isospin breaking due to the  $K^+ - K^0$  mass

difference, the mixing of the  $f_0(980) - a_1(980)$  masses and of the  $f_0$  states, we have somewhat violated one of the conditions of the "elastic" 2-channel unitarity, namely, the third condition, provided the first two are satisfied. In Table 3 the obtained parameter values of poles on sheets  $L_1$  and  $L_{12}$  are cited on the complex energy plane ( $\sqrt{s_r} = E_r - i\Gamma_r/2$ ). The value  $\chi^2/\text{ndf} \approx 1.04$  in the analysis from the threshold to 1.89 GeV is obtained if from 157 used experimental points one rejects three points at energies 0.285, 0.3656 and 0.730 GeV which give an anomalously large contribution to  $\chi^2$ . The description of the phase

Table 3.

Energy region	Sheet	$f_0(980)$		$f_0(1500)$		$\chi^2/\text{ndf}$
		$E, \text{MeV}$	$\Gamma, \text{MeV}$	$E, \text{MeV}$	$\Gamma, \text{MeV}$	
0,6-1,89 GeV	$L_1(\text{II})$	$1000 \pm 5$	$48 \pm 6$	$1552 \pm 15$	$494 \pm 35$	1,00
	$L_{12}(\text{III})$	$971 \pm 8$	$152 \pm 15$	$1516 \pm 15$	$369 \pm 32$	
0,28-1,89 GeV	$L_1(\text{II})$	$996 \pm 2$	$53 \pm 3$	$1640 \pm 22$	$720 \pm 34$	1,32
	$L_{12}(\text{III})$	$1352 \pm 12$	$857 \pm 46$	$1551 \pm 14$	$751 \pm 38$	

shift  $\delta_0^0$  is practically the same in both the analyses (the curve in the first analysis starts at 0.6 GeV and actually is laid on the depicted one), however, the elasticity-parameter description seems to be somewhat worse in the second analysis (Fig.2). It should be pointed out that the pole cluster of the  $f_0(980)$  resonance is somewhat eroded, although the quality of description is approximately the same in both the analyses and the second describes satisfactorily the phase shift also near the threshold.

On the basis of formulae (15) with the parametrization (18) and (19), one can obtain the predictions for coupled processes of the  $K\bar{K}$  scattering and  $\pi\pi \rightarrow K\bar{K}$ . In this case, using the  $d_B$ -function (18) assumes that the background of the isoscalar  $s$ -wave  $K\bar{K}$  scattering is completely defined by the background of the  $\pi\pi$  scattering. In the first approximation this supposition turns out to be reasonable, whereas in the enlarged analysis of the data on these coupled processes a more detailed description may be required [6].

So, we have satisfactorily predicted the behaviour of the  $s$ -wave of the  $\pi\pi \rightarrow K\bar{K}$



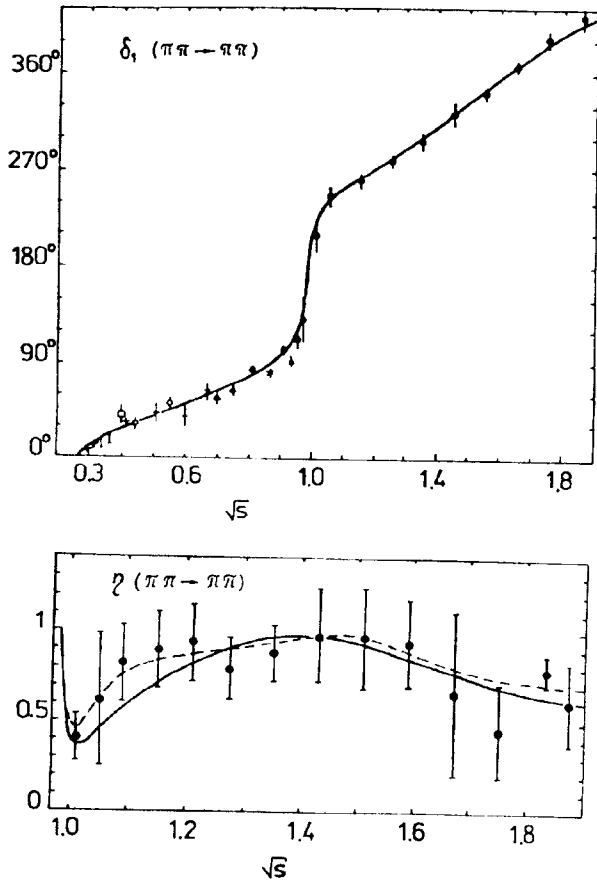


Fig.2: The energy dependences of the phase shift ( $\delta_1 \equiv \delta_0^0$ ) of the amplitude and of the elasticity parameter ( $\eta$ ) in the scalar-isoscalar channel obtained on the basis of the experimental data processing in the regions from 0.6 to 1.89 GeV (dashed curve) and from the  $\pi\pi$ -threshold to 1.89 GeV (solid curves). In the figure only certain typical experimental points are depicted.

process approximately up to 1.25 GeV (see Fig.3: experimental points are taken from works [25]-[27]). However, above 1.25 GeV, a considerable deviation from the experimental data in the prediction for this process is seen where the influence of the  $\eta\eta$  channel begins to be noticeable. This indicates the necessity of explicit consideration of the  $\eta\eta$  threshold. Note also that the prediction on the basis of the second analysis gives the overestimated values for  $|S_{12}|$  even in the region from the  $K\bar{K}$  threshold to 1.2 GeV. However, a definite success in the description of the  $\pi\pi \rightarrow K\bar{K}$  process on the basis of the first analysis gives a chance to determine the constants of the  $f_0(980)$  coupling with the  $\pi\pi$  and  $K\bar{K}$  systems through the residue of amplitudes at the pole on the sheet  $L_1$ . Expressing the  $T$ -matrix via the  $S$  matrix as

$$\mathbf{S} = I + 2i\rho^{1/2}\mathbf{T}\rho^{1/2}, \quad (20)$$

we write down the analytical continuations of their elements to  $L_1$  in terms of them on the physical sheet  $L_0$ :

$$T_{11}^{(1)} = \frac{T_{11}^{(0)}}{S_{11}^{(0)}}, \quad T_{22}^{(1)} = T_{22}^{(0)} - 2i\rho_1 \frac{(T_{12}^{(0)})^2}{S_{11}^{(0)}}, \quad T_{12}^{(1)} = \frac{T_{12}^{(0)}}{S_{11}^{(0)}}. \quad (21)$$

Then, taking account of (21), we obtain

$$\frac{g_{\pi\pi f_0}^2}{4\pi} = |\rho_1(z_1^{*-1})|^{-1} \frac{8q_z^2}{|z_1|^2} \left| \lim_{z \rightarrow z_1^{*-1}} (1 - z_1^* z)(1 + z_1 z) S_{11} \right| \quad (22)$$

For calculating  $g_{K\bar{K}f_0}$  it is convenient to use the amplitude  $T_{22}$ ; then from the second expression (21) it is seen that the desired residue is proportional to  $(g_{\pi\pi f_0} g_{K\bar{K}f_0})^2$ , i.e.

$$\frac{g_{\pi\pi f_0}^2}{4\pi} \frac{g_{K\bar{K}f_0}^2}{4\pi} = |\rho_1(z_1^{*-1})\rho_2(z_1^{*-1})|^{-1} \left( \frac{8q_\pi^2}{|z_1|^2} \right)^2 \left| \lim_{z \rightarrow z_1^{*-1}} (1 - z_1^* z)(1 + z_1 z) S_{22} \right|. \quad (23)$$

On the basis of formulae (22) and (23), the following values of the coupling constants were obtained:

$$\frac{g_{\pi\pi f_0}^2}{4\pi} \approx 0.8 \text{ GeV}^2, \quad \frac{g_{K\bar{K}f_0}^2}{4\pi} \approx 3,164 \text{ GeV}^2. \quad (24)$$

i.e.  $g_{\pi\pi f_0}/g_{K\bar{K}f_0} \approx 0,52$ , which corresponds to both the  $qq\bar{q}\bar{q}$  nature of  $f_0(980)$  [8]-[10] and the unitarized  $qq$  model [12].

## 2. The 3-channel approach.

Above we have already concluded that it is necessary to consider explicitly the  $\eta\eta$  thresh-

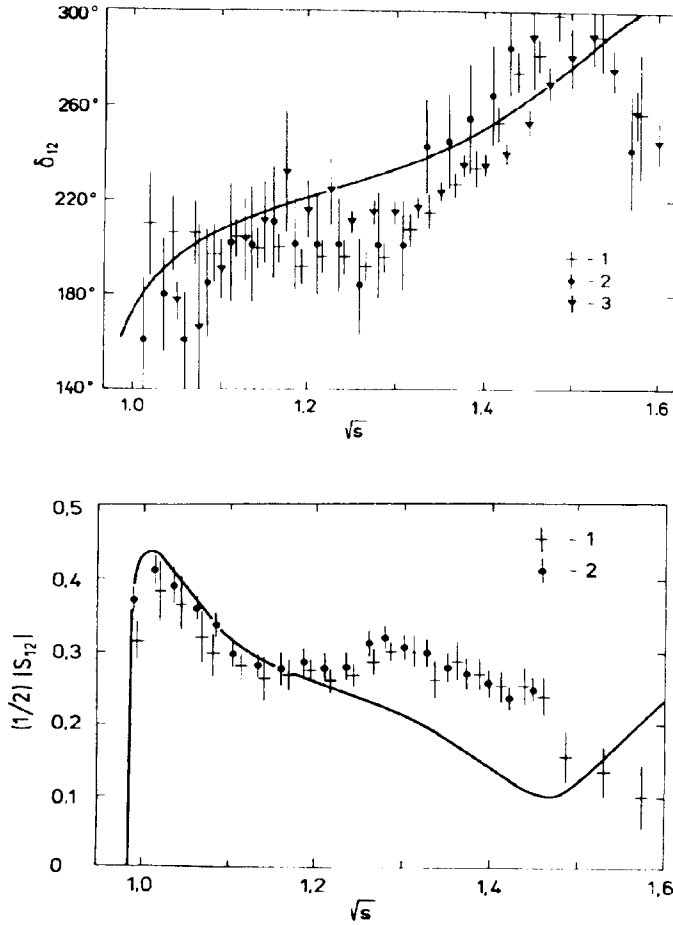


Fig.3: Predictions for the phase ( $\delta_{12}$ ) and the modulus of the isoscalar  $s$  wave matrix element of the  $\pi\pi \rightarrow K\bar{K}$  process as compared with the experimental data (1 - [25], 2 [26], 3 - [27]).

old that slightly affects the parameters of the  $f_0(975)$  resonance (though gives further information on it); however, it is of vital importance for higher-lying resonances.

Since in the 3-channel consideration it is impossible to map the 8-sheeted Riemann surface onto a plane with the help of a simple function, we construct a 4-sheeted model of the Riemann surface approximating the initial Riemann surface in accordance with our approach of a consistent account of the nearest singularities on all the relevant Riemann sheets. We neglect the influence of the  $\pi\pi$ -threshold branch point (however, unitarity on the  $\pi\pi$  cut is taken into account). In this case, the uniformizing variable can be chosen as

$$w = (k_2 + k_3)/(m_\eta^2 - m_K^2)^{1/2}. \quad (25)$$

It maps the model of the 8-sheeted Riemann surface onto the  $w$ -plane (Fig.4), divided

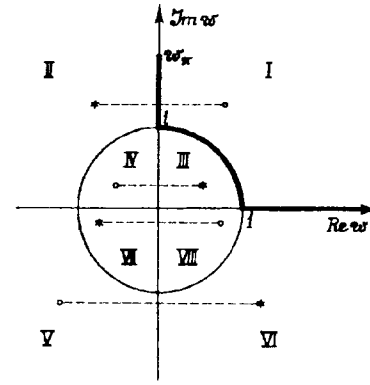


Fig.4:  $w$ -plane. The Roman numerals (I,II,...,VIII) denote the images of the corresponding sheets of the Riemann surface; the thick line represents the physical region (the points  $w_\pi$ ,  $i$  and  $1$  are the  $\pi\pi$ ,  $K\bar{K}$  and  $\eta\eta$  thresholds, respectively). The depicted positions of poles (\*) and of zeros (o) give the representation of the type (a) resonance in  $S_{11}$ . The dashed lines indicate a "pole-zero" symmetry required for elastic unitarity in the  $(w_\pi, i)$ -region.

into two parts by a unit circle centered at the origin. The sheets  $L_0$  ( $L_{12}$ ),  $L_1$  ( $L_2$ ),  $L_{23}$  ( $L_{13}$ ) and  $L_{123}$  ( $L_3$ ) are mapped onto the exterior (interior) of the unit disk in the 1st, 2nd, 3rd and 4th quadrants, respectively. The physical region extends from the point  $w_\pi$  on the imaginary axis ( $\pi\pi$  threshold,  $|w_\pi| > 1$ ) down this axis to the point  $i$  on the unit circle ( $K\bar{K}$  threshold), further along the unit circle clockwise in the 1st quadrant to point  $1$  on the real axis ( $\eta\eta$  threshold) and then along the real axis to  $\infty$ . The type (a) resonance is represented in  $S_{11}$  by the pole on the images of  $L_1$ ,  $L_{12}$ ,  $L_{123}$  and  $L_{13}$  and by zeros symmetric to these poles with respect to the imaginary axis. The last "pole-zero"

symmetry is required for elastic unitarity on the  $(w_{\pi, i})$ -interval. In Fig. 4 our notation for the sheets of the Riemann surface by the Roman numerals is used.

The Le Coultre-Newton relations are somewhat modified with taking account of the used model of the Riemann surface (note that on the  $w$ -plane the points  $w_0, w_0^{-1}, -w_0, w_0^{-1}$  correspond to the  $s$ -variable point  $s_0$  on sheets  $L_0(I), L_2(IV), L_2(IV), L_2(III)$  respectively):

$$\begin{aligned} S_{11} &= \frac{d^*(-w^*)}{d(w)}, & S_{22} &= \frac{d(-w^{-1})}{d(w)}, & S_{33} &= \frac{d(w^{-1})}{d(w)}, \\ D_{33} &= \frac{d^*(w^{*-1})}{d(w)}, & D_{22} &= \frac{d^*(-w^{*-1})}{d(w)}, & D_{11} &= \frac{d(-w)}{d(w)}. \end{aligned} \quad (26)$$

Since the used model Riemann surface means only the consideration of the semi sheets of the initial Riemann surface nearest to the physical region, then in this case there is no point in saying for the property of the real analyticity of the amplitudes. The 3 channel unitarity requires the following relations to hold for physical  $w$  values:

$$|d(-w^*)| \leq |d(w)|, \quad |d(-w^{-1})| \leq |d(w)|, \quad |d(w^{-1})| \leq |d(w)|. \quad (27)$$

$$|d(w^{*-1})| = |d(-w^{*-1})| = |d(-w)| = |d(w)|. \quad (28)$$

Taking the  $d$ -function as  $d = d_B d_{res}$  where the resonance part has the form:

$$d_{res}(w) = w^{2M} \prod_{r=1}^M \prod_{i=1}^4 (w + w_{r_i}^*) \quad (29)$$

( $M$  is the number of resonances;  $-w_{r_i}^*$  ( $i = 1, \dots, 4$ ) are pole positions, corresponding to the type (a) resonance) it is easy to obtain expressions for the matrix elements.

On the basis of formulae (26) and (29) we analysed all available data on the isoscalar  $s$ -wave  $\pi\pi$  scattering in the energy region 0.7-1.6 GeV [5] with taking account of  $K\bar{K}$  and  $\eta\eta$  thresholds. The background was taken in the elastic form:

$$S_{11}^B = e^{2i\delta^B(s)}, \quad \delta^B(s) = a + b\sqrt{s}$$

(from the analysis:  $a = -1,376 \pm 0,056$ ,  $b = 0,6 \pm 0,0025$ ).

Satisfactory description ( $\chi^2/ndf \approx 1.12$  if the point at 0.91 GeV that gives an anomalously large contribution to  $\chi^2$  is rejected) of experimental data is achieved for the phase shift and the elasticity parameter with two resonances (Fig.5). The pole positions of resonances

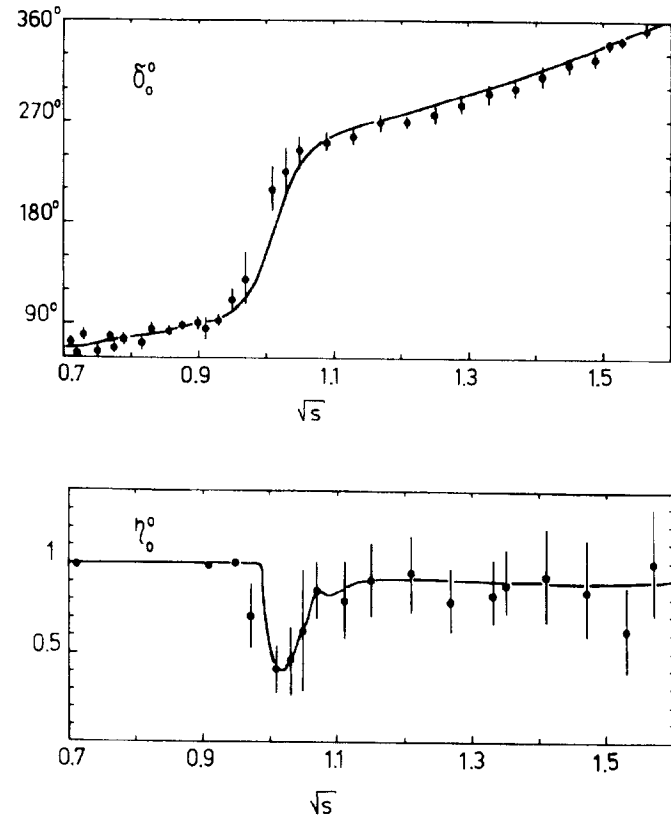


Fig.5: The phase shift and the elasticity parameter of the scalar-isoscalar channel of the  $\pi\pi$  scattering obtained on the basis of the  $\chi^2$  analysis of the experimental data. Separate characteristic experimental points are depicted.

on different sheets in the energy plane ( $\sqrt{s_r} = E_r - i\Gamma_r/2$ ) are presented in Table 4. Note that the parameters of the  $f_0(980)$  meson were changed somewhat as compared

Table 4.

Sheet	$f_0(980)$		$f_0(1500)$	
	$E, \text{MeV}$	$\Gamma, \text{MeV}$	$E, \text{MeV}$	$\Gamma, \text{MeV}$
$L_1(\text{II})$	$1017 \pm 5$	$35 \pm 7$	$1496 \pm 16$	$548 \pm 35$
$L_{12}(\text{III})$	$1031 \pm 16$	$128 \pm 30$	$1156 \pm 36$	$146 \pm 13$
$L_{123}(\text{VI})$	$1025 \pm 8$	$23 \pm 10$	$1502 \pm 20$	$614 \pm 40$
$L_{13}(\text{VII})$	$1139 \pm 60$	$108 \pm 42$	$1147 \pm 55$	$145 \pm 62$

to our 2-channel analysis [4] (to make the  $f_0(980)$  cluster more compact). As is already discussed in work [4], this should not influence the qualitative conclusion about the  $f_0(980)$  nature but shows a rather strong coupling of this resonance with the  $\eta\eta$  system and the importance of taking account of the  $\eta\eta$ -channel influence to obtain the reliable values of the  $f_0(980)$  parameters. The considerable coupling of the  $f_0(980)$  meson with the  $\eta\eta$  system can manifest itself experimentally, e.g., in crossing processes, such as  $\pi\eta$  and  $K\eta$  scattering, in the exchanges of this meson. The considerable shift of the  $f_0(980)$  pole on sheet  $L_{13}$  is stipulated by a great coupling between  $\pi\pi$  and  $\eta\eta$  channels whereas the coupling between  $\pi\pi$  and  $K\bar{K}$  channels is suppressed strongly by the phase-space volume (owing to proximity of the  $f_0(980)$  mass to the  $K\bar{K}$  threshold) whereby it is accounted for a smaller shift of the pole on  $L_{12}$ . A displacement of the pole on  $L_{123}$ , related with influence of the  $\eta\eta$  channel, is compensated by the effect of coupling between the  $K\bar{K}$  and  $\eta\eta$  channels which displaces the pole to the opposite direction (which is explained by the corresponding signs of the channel momenta when continuing onto sheet  $L_{123}$ ). Many authors have already noted that the  $f_0(980)$  width cited in tables [1] is a visible one, the total width of this resonance is  $\sim 500$  MeV.

As to the second resonance, which we denoted symbolically as  $f_0(1500)$ , the analysis of experimental data shows obviously a resonance manifestation. To discuss really its parameters, one must explicitly take account of the  $\eta\eta'$  threshold (and possibly  $\rho\rho$  and

$\omega\omega$ ). Notice also that this analysis does not reveal the  $f_0(1590)$  resonance by virtue of its comparatively weak coupling with the  $\pi\pi$  channel though, of course, this resonance must affect the results due to its rather considerable couplings with the  $\eta\eta$  and  $\eta\eta'$  channels. Other scalar resonances in the considered energy region (if they exist) should have a relatively weak coupling with the  $\pi\pi$  system, i.e. they should be described by clusters without zeros on the sheet  $L_0$  in  $S_{11}$ .

Note that processing experimental data we ensured the fulfilment of the unitarity conditions (27) allowing certain violations in conditions (28). This breakdown of the "elastic" 3-channel unitarity results in additional branch points in the matrix elements  $S_{ij}$  ( $i \neq j$ ) outside of the physical region but it gives a chance to take into account effectively the influence of effects not included explicitly and to avoid the appearance of fictitious states. Notice that if one disregards the  $\eta\eta$  threshold, i.e. sheets  $L_{23}$ ,  $L_{123}$ ,  $L_{13}$  and  $L_3$ , then poles on the neglected sheets  $L_{13}$  and  $L_{123}$  turn out to lie on  $L_1$  and  $L_{12}$ , respectively, imitating a supplementary state [3].

## 4 CONCLUSIONS

In the present work, the multichannel approach to studying resonances in the coupled processes is given with the aim of determining their QCD nature. The  $N$ -channel formalism (and, as examples, 2- and 3-channel) is presented, the more so as in the approach of the consistent account of the nearest (to the considered physical region) singularities on all the Riemann sheets an  $N(> 3)$ -channel problem always can be effectively reduced to the 2- and 3-channel problem. The given consideration is required because it gives a possibility to apply such first principles, as analyticity and unitarity, immediately to analyzing the experimental data and, as a consequence, to obtain a model-independent information on multichannel resonances and their coupling constants. The formula of analytical continuation of the  $N$ -channel  $S$ -matrix to the unphysical sheets of the Riemann surface is given which is a solution of the  $N$ -channel problem in the sense of offering a chance to predict (on the basis of analysis of one process) the coupled-process amplitudes on the uniformization plane of the  $S$ -matrix at a certain conjecture about the background. Another possibility to have such a solution of the  $N$ -channel is the Le Couteur – New-

ton relations [22] used also in this work. This is demonstrated for the 2- and 3-channel problems.

The resonance representations by pairs of complex-conjugate clusters of poles and zeros on the Riemann surface are discussed, and the conception of standard clusters as model-independent characteristics of the resonance is developed. The fact that the phase shift crosses the value  $n\pi/2$  is not a sufficient condition for the state existence (an example is the old  $\epsilon(750)$ ). This condition provides the description in terms of one of standard clusters. The cluster kind is determined by the analysis of experimental data and seems to be related to the nature of a resonance. Falling out a pole (or poles) from a cluster in the analysis requires a further explicit consideration of some effects. It is shown that the pole-cluster representation gives not only a qualitative characteristic of the resonances but also a chance of a quantitative description of the coupled-process amplitudes. In this case all the complications of the analytical structure related with a finite width of resonances and with the influence of crossing channels and of high-energy “tails” are accumulated in a quite smooth background, at least, in the scalar sector of the pseudoscalar mesons scattering.

Both open and closed channels participate in forming the resonance pole clusters. It is shown that the neglect of the important (even energetic-closed) channel in the Riemann surface structure gives rise to the imitation of supplementary states of a sometimes unfamiliar nature (such as a glueball); in the (practically used in analyses) reduced  $K$ -matrix [21] this leads to an additional pole on the real axis. Note that depending on the cluster type the resonance may be represented in the  $K$ -matrix also by poles more than one (for example, when zeros on the physical sheet are in  $S$ -matrix elements of two coupled processes, by two poles on the real axis). To distinguish these cases, one must study the pole arrangement on the Riemann surface. The multisheeted structure of the Riemann surface is taken into account through the choice of proper uniformizing variables.

The method is exemplified with the isoscalar  $s$ -wave channel of coupled processes  $\pi\pi \rightarrow \pi\pi, K\bar{K}$  and scalar resonances. It is shown that for a physically satisfactory description of these processes in the energy region below 1.5 GeV, the  $\eta\eta'$  threshold must be taken into account explicitly. In the 2- and 3-channel considerations of the  $\pi\pi$  scattering

in the energy region 0.6-1.89 GeV and 0.7-1.6 GeV, respectively, two resonances ( $f_0(980)$  and  $f_0(1500)$ ) turned out to be sufficient. The obtained values of the  $f_0(975)$  coupling constants with the  $\pi\pi$  and  $K\bar{K}$  systems correspond to the  $qq\bar{q}\bar{q}$  nature of  $f_0(975)$  [8, 9] or the unitarized  $qq$  model [12]. To discuss the  $f_0(1500)$  parameters, one must explicitly take into account at least the  $\eta\eta'$  threshold. Other scalar resonances in the considered energy region should have a relatively weak coupling with the  $\pi\pi$  system, i.e. they should be described by clusters without zeros on the sheet  $L_0$  in  $S_{11}$ .

A few words also about the conjectural scalar state below 900 MeV. A relatively recent amplitude analysis [28] of data on the  $\pi^+n_1 \rightarrow \pi^+\pi^-p$  process suggests the existence of the scalar meson with a mass 750 MeV and a width of 100-150 MeV. Models of the Nambu–Jona-Lasinio type (see, e.g., [29, 30]) also predict a meson with mass  $\sim 700$ , admittedly, very wide. It is amusing that if this object were identified as a glueball, then its  $\pi\pi$  width according to the Ellis-Lanik formula [31] obtained in an approach similar to the NJL approach would be  $\sim 150$  MeV. Our analyses do not see this state. Evidently, it is worth to carry out a special analysis with an explicit account of the near left-hand branch point.

It seems also that the described test of the resonance presence must be applied to a number of particle sectors, above all, to the scalar one at higher energies.

Note in conclusion that the pole-cluster representation of resonances was used also in studying nucleon isobars in work [32].

## Acknowledgments

One of the authors (V.A.M.) would like to thank the International Centre for Theoretical Physics, Trieste, for hospitality.

This work was supported by the Russian Fund for Fundamental Research (Grant No.93-02-03807).

## References

- [1] Particle Data Group, Phys. Rev. **D50**, 1173 (1994).
- [2] D. Krupa, V.A. Meshcheryakov and Yu.S. Surovtsev, Yad. Fiz. **43**, 231 (1986).
- [3] D. Krupa, V.A. Meshcheryakov and Yu.S. Surovtsev, Problems on High Energy Physics and Field Theory, Proc. IX Workshop, Protvino, 1986. Moscow: Nauka, 1987, P.335.
- [4] D. Krupa, V.A. Meshcheryakov and Yu.S. Surovtsev, Czech. J. Phys. **B38**, 1129 (1988).
- [5] D. Krupa, V.A. Meshcheryakov and Yu.S. Surovtsev, Yad. Fiz. **54**, 1112 (1991).
- [6] D. Krupa, V.A. Meshcheryakov and Yu.S. Surovtsev, Yad. Fiz. **58**, 1672 (1995).
- [7] F.E. Close, Yu.L. Dokshitzer, V.N. Gribov, V. Khose and M.G. Ryskin, Phys. Lett. **B319**, 291 (1993).
- [8] R.L. Jaffe, Phys. Rev. **D15**, 267, 281 (1977).
- [9] N.N. Achasov, S.A. Devyanin and G.N. Shestakov, Phys. Lett. **B96**, 168 (1980). Z. Phys. **C22**, 53 (1984).
- [10] A.E. Dorokhov, Yu.A. Zubov and N.I. Kochelev, Yad. Fiz. **50**, 171 (1989). JINR Commun. E2-89-867, Dubna, 1989.
- [11] R.L. Jaffe, Phys. Lett. **41**, 271 (1975). D. Robson, Nucl. Phys. **B130**, 328 (1977).
- [12] N. Törnqvist, Phys. Rev. Lett. **49**, 624 (1982).
- [13] J. Lanik, Phys. Lett. **B306**, 139 (1993).
- [14] J. Lanik, Z. Phys. **C39**, 143 (1988).
- [15] M. Majewski, Z. Phys. **C39**, 121 (1988).
- [16] J. Weinstein J. and N. Isgur, Phys. Rev. **D27**, 588 (1983); *ibid.* **D41**, 2236 (1990).
- [17] F. Cannata, J.P. Dedonder and L. Leśniak, Phys. Lett. **B207**, 115 (1988).
- [18] K.L. Au, D. Morgan and M.R. Pennington, Phys. Rev. **D35**, 1633 (1987).
- [19] D. Morgan and M.R. Pennington, Phys. Rev. **D48**, 1185 (1993).
- [20] M. Kato, Ann. Phys. **31**, 130 (1965).
- [21] R.H. Dalitz, Rev. Mod. Phys. **33**, 471 (1961).
- [22] K.J. Le Couteur K.J., Proc. Roy. Soc. **A256**, 115 (1960). R.G. Newton, J. Math. Phys. **2**, 188 (1961).
- [23] B. Hyams et al., Nucl. Phys. **B64**, 134 (1973); *ibid.*, **B100**, 205 (1975).
- [24] A. Zylbersztejn et al., Phys. Lett. **B38**, 457 (1972). P. Sonderegger and P. Bonamy, Proc. 5th Intern. Conf. on Elementary Particles, Lund, 1969, paper 372. J.R. Bensinger et al., Phys. Lett. **B36**, 134 (1971). J.P. Baton et al., Phys. Lett. **B33**, 525, 528 (1970). P. Baillon et al., Phys. Lett. **B38**, 555 (1972). L. Rosselet et al., Phys. Rev. **D15**, 574 (1977). A.A. Kartamyshev et al., Pis'ma v Zh. Eksp. Teor. Fiz. **25**, 68 (1977). A.A. Bel'kov et al., Pis'ma v Zh. Eksp. Teor. Fiz. **29**, 652 (1979).
- [25] A.B. Wicklund et al., Phys. Rev. Lett. **45**, 1469 (1980). D. Cohen et al., Phys. Rev. **D22**, 2595 (1980).
- [26] A.D. Martin and E.N. Ozmutlu, Nucl. Phys. **B158**, 520 (1977).
- [27] A. Etkin et al., Phys. Rev. **D25**, 1786 (1982).
- [28] M. Svec, A. de Lesquen and L. van Rossum, Phys. Rev. **D45**, 55 (1992).
- [29] M.K. Volkov, Ann. Phys. **157**, 282 (1984). M. Nagy, U.S. Suyarov and M.K. Volkov, JINR Rapid Communication N° 25-87, Dubna, 1987, p. 11.
- [30] K. Kusaka, M.K. Volkov and W. Weise, Phys. Lett. **B302**, 145 (1993).
- [31] J. Ellis and J. Lanik, Phys. Lett. **B150**, 289 (1985); *ibid.* **B175**, 83 (1986).
- [32] R.E. Cutkosky and S. Wang, Phys. Rev. **D42**, 235 (1990).

